4.8.2 Dead-Time Correction

The data acquisition system was not able to detect all particles. Once the MAIN-OR was triggered, it was not able to trigger again on any signal arriving within the following 32 ns. Also, only the first four MAIN-OR signals of each spill could be analyzed by the ADC modules.[17] For illustration let us consider the measurement of $A_{\|}$ at large x values. The cross-section is here bigger for spills with antiparallel beam and target helicities than for spills with parallel helicities. Exactly this difference led to our measured asymmetry. But spills with more events (helicity antiparallel) had a bigger dead-time and therefore relatively more events were lost than for spills with less events (helicity parallel). The dead-time effect therefore reduced the measured asymmetry, and the dead-time correction corrected for this reduction.

While analyzing each run, the number of spills N_i with $i = 0, 1, 2, \ldots 16$ or more triggers were recorded (from TDC measurements). Practically no spill had 12 or more MAIN-ORs, therefore the upper limit of 16 hits per spill was sufficient. The measured number of fully recorded MAIN-OR events was

$$N_{\text{meas}} = \sum_{i=0}^{16} \bar{i} N_i, \tag{144}$$

where $\bar{i} = i$ for $i \leq 4$ and $\bar{i} = 4$ for $i > 4$.

The real number of MAIN-OR events for this run were then estimated via a matrix P obtained from a simple Monte Carlo simulation. It was assumed that the triggers were randomly distributed within the spill time of 2.2 μs, that the dead-time was 32 ns, and that not more than 16 triggers appeared within the spill. The matrix connected the number of real events with the number of measured events. For example, the matrix elements $P_{n,m}$ stood for the probability that n real triggers lead to m measured triggers. Of course, $\sum_{m=1}^{n} P_{n,m} = 1$. From this, we were able to estimate the total number of real events:

$$N_{\text{real}} = \sum_{n=1}^{16} n \sum_{m=1}^{16} N_m P^{-1}_{n,m} \tag{145}$$

[17] Strictly speaking, this "four-per-pulse" limitation was not due to dead-time problems, but we still include it under the name "dead-time".

The dead-time coefficient was then

$$d = \frac{N_{\rm real}}{N_{\rm meas}} > 1. \tag{146}$$

Separate dead-time corrections d_L and d_R were calculated for each run, spectrometer and beam polarization sign, and were applied to the recorded number of events $N_L^{\rm raw}$ and $N_R^{\rm raw}$ per x and Q^2 bin. Dividing then by the charge Q_L and Q_R of the incoming electrons, one obtained the rates N_L and N_R from Eq. (143):

$$N_L = \frac{d_L N_L^{\rm raw}}{Q_L} \qquad \text{and} \qquad N_R = \frac{d_R N_R^{\rm raw}}{Q_R} \tag{147}$$

Fig. 33 shows the dead-times for the deuteron 29 GeV runs. The horizontal axis lists the average number of MAIN-OR triggers (as detected by the TDCs) per number of spills.

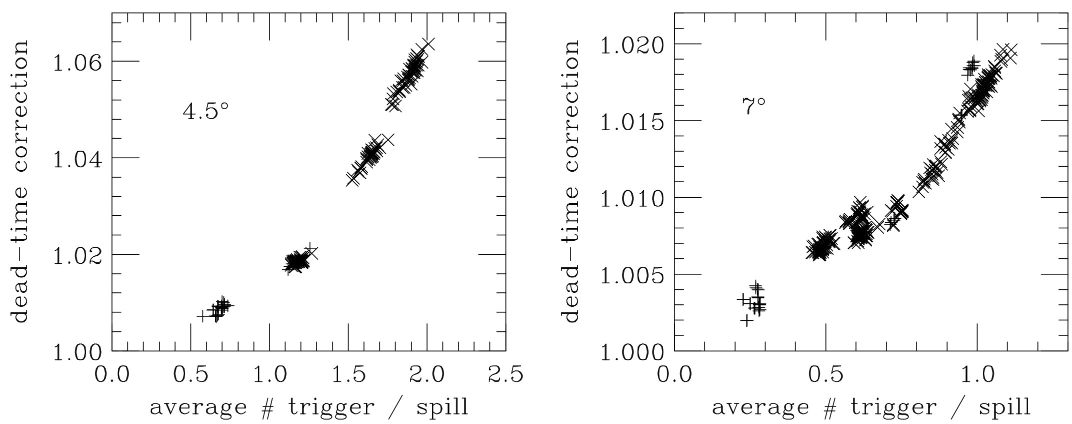

Figure 33 Dead-times for 29 GeV deuteron runs. Included are both longitudinal and transverse runs. The symbol "×" denotes electron runs, the symbol "+" positron runs. To the left are the values for the 4.5° spectrometer, to the right the values for the 7° spectrometer.

The 4.5° dead-time corrections were around $d_{L,R} \approx 1.05$, while the 7° dead-time corrections were considerably lower, around $d_{L,R} \approx 1.015$, due to the decreased rate in that spectrometer. They increased the integral of g_1 over the measured x-region by about 2% for the 29 GeV data. The positron run dead-times (with symbol + in Fig. 33) had a very low rate, but still, some of them had a high dead-time in the 7° spectrometer. No plausible explanation exists for this, but the influence of these runs on the data is negligible.